

Electronic supplementary information

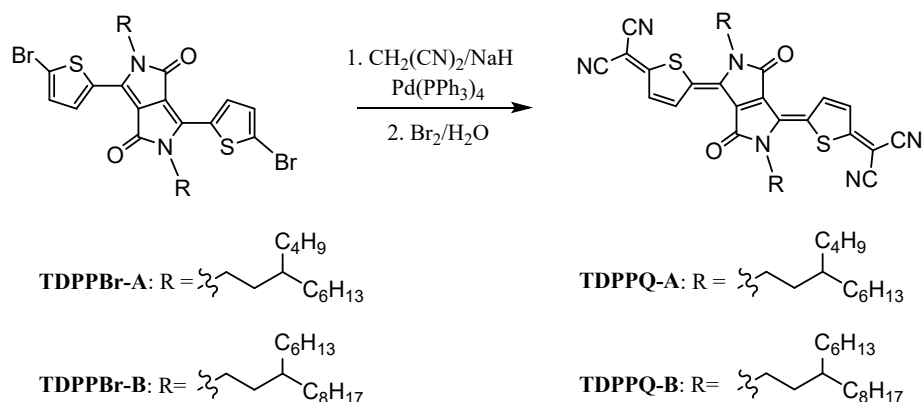
High-Mobility and Nonhalogenated-Solvent-Processable n-Type Organic Semiconductors Enabled by Alkyl-Side-Chain Engineering

Sihong Pan^{†a}, Zhen Ji^{†b}, Zhikang Zhang^{†a}, Junwen Yang^a, Jiahao Yang^a, Zhongmin Zhou^{*c}, Liyao Liu^b, Chao Wang^{*a}, Chong-an Di^b

General procedures

All chemicals were purchased from commercial suppliers and used without further purification. All air-sensitive reactions were performed under N₂ by Schlenk techniques. ¹H and ¹³C NMR spectra were recorded on a 400 MHz spectrometer (JNM-ECZ400S/L, JEOL). NMR data are presented as follows: chemical shift in ppm (δ), multiplicity (s = singlet, d = doublet, t = triplet, and m = multiplet), coupling constant in Hz, and integration. HRMS was carried out on a mass spectrometer (JMS-T100GCV, JEOL). TGA was performed on a thermal gravimetric analyzer under N₂ at a heating rate of 10 °C min⁻¹, heating from room temperature to 500 °C. DSC was conducted on a differential scanning calorimeter under an N₂ flow at a heating rate of 10 °C min⁻¹ in a temperature range from room temperature to 250 °C. The UV-vis absorption spectra were recorded on a spectrophotometer (V-570, JASCO). CV measurements were carried out on a CHI660C analyzer with a three-electrode cell equipped with a platinum disk working electrode, a platinum wire counter electrode, and a Ag/AgCl reference electrode under N₂ atmosphere. The supporting electrolyte was an anhydrous dichloromethane solution with 0.1 M tetrabutylammonium hexafluorophosphate. AFM images were recorded on a scanning probe microscope (Bruker Dimension Icon) in tapping mode. GIWAXS measurements were performed with a wavelength of 0.10002 nm. All thin films were irradiated at a fixed angle of 0.12°.

Synthesis and Characterization



The precursors TDPPBr-A and TDPPBr-B were synthesized according to literature procedure [S1, S2].

Synthesis of TDPPQ-A. Sodium hydride (60% in oil, 0.096 g, 2.4 mmol) was added to a degassed solution of malononitrile (0.079 g, 1.2 mmol) in anhydrous dimethoxyethane (10 mL) at 0 °C under an argon atmosphere, and the resulting suspension was stirred at room temperature for 30 min to give rise to a solution of malononitrile anion. TDPPBr-A (0.412 g, 0.5 mmol) and tetrakis-(triphenylphosphine)palladium (0.116 g, 0.1 mmol) were dissolved in dimethoxyethane (10 mL), and then the mixture was heated under reflux for 20 min, followed by the slow addition of the prepared malononitrile anion solution by a syringe. The mixture was refluxed for 6 h and then treated with saturated bromine water (20 mL) at 0 °C. After stirring for 1 h at room temperature, the mixture was extracted with chloroform (50 mL × 4). The combined organic layer was washed with brine and dried over MgSO_4 . After evaporation of the solvent, the residue was purified by column chromatography on silica gel with dichloromethane/hexane (3:2), followed by recrystallization from chloroform/methanol to give TDPPQ-A as a dark-green solid (0.245 g, 62%). ^1H NMR (400 MHz, CDCl_3): δ 9.38 (d, $J = 5.6$ Hz, 2H), 7.38 (d, $J = 5.6$ Hz, 2H), 4.07 (t, $J = 7.7$ Hz, 4H), 1.62–1.68 (m, 4H), 1.27–1.48 (m, 34H), 0.86–0.92 (m, 12H). ^{13}C NMR (100 MHz, CDCl_3): δ 172.6, 161.1, 146.9, 135.4, 133.3, 131.5, 130.5, 113.2, 112.4, 71.4, 41.7, 36.0, 34.1, 33.5, 31.9, 29.7, 28.9, 26.7, 23.1, 22.8, 14.2. HRMS (FD) m/z calcd. for $\text{C}_{46}\text{H}_{58}\text{N}_6\text{O}_2\text{S}_2$: 790.40626, found: 790.40621.

Synthesis of TDPPQ-3. TDPPQ-3 was prepared according to the same procedure as that for TDPPQ-A

in 52% yield. ^1H NMR (400MHz, CDCl_3): δ 9.38 (d, $J = 5.6$ Hz, 2H), 7.38 (d, $J = 5.6$ Hz, 2H), 4.07 (t, $J = 7.7$ Hz, 4H), 1.62–1.68 (m, 4H), 1.27–1.48 (m, 50H), 0.85–0.89 (t, $J = 6.4$ Hz, 12H). ^{13}C NMR (100 MHz, CDCl_3): δ 172.6, 161.1, 146.9, 135.4, 133.3, 131.5, 130.5, 113.2, 112.4, 71.4, 41.7, 36.0, 34.1, 33.5, 31.9, 30.0, 29.7, 29.4, 26.7, 22.8, 14.2. HRMS (FD) m/z calcd. for $\text{C}_{54}\text{H}_{74}\text{N}_6\text{O}_2\text{S}_2$: 902.53146, found: 902.53118.

Supplementary data

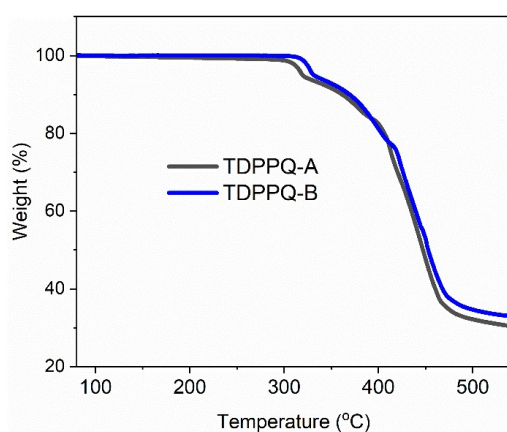


Figure S1. TGA curves of TDPPQ-A and TDPPQ-B.

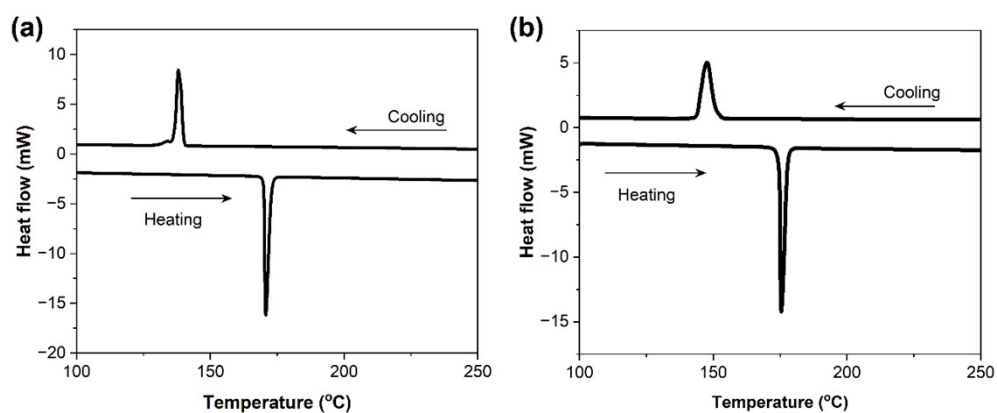


Figure S2. DSC curves of (a)TDPPQ-A and (b) TDPPQ-B.

Table S1. The Hansen solubility parameters of different organic solvents and the solubility values of

TDPPQ-A and TDPPQ-B in these solvents (TDPPQ-3^[S1] is used as a reference).

Solvent	Hansen solubility parameters (MPa ^{1/2}) [S3, S4]			Solubility of TDPPQ-A (mg mL ⁻¹)	Solubility of TDPPQ-B (mg mL ⁻¹)	Solubility of TDPPQ-3 (mg mL ⁻¹)
	δ_D	δ_P	δ_H			
Chloroform (CF)	17.8	3.1	5.7	17.0	18.5	17.6
2-Methyltetrahydrofuran (2-MTHF)	16.4	4.8	4.9	11.1	9.2	2.4
Acetone (AT)	15.5	10.4	7.0	6.3	4.1	0.3

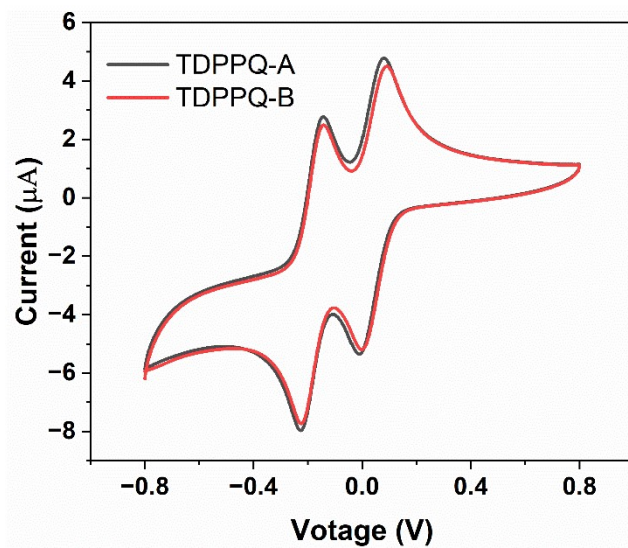


Figure S3. CV of TDPPQ-A and TDPPQ-B.

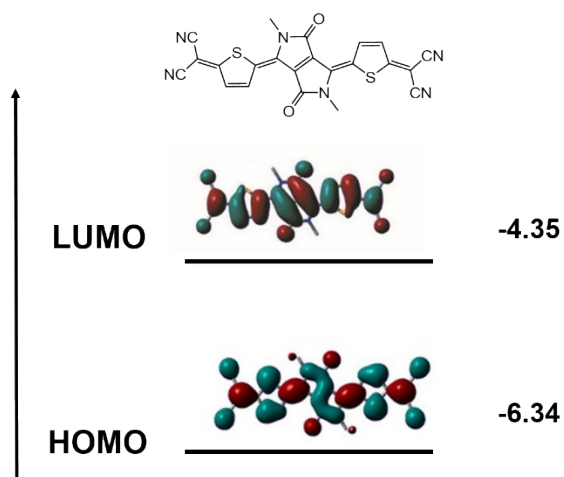


Figure S4. Electronic density contours of HOMO and LUMO orbitals of TDPPQs.

Table S2. Optical absorption data, electrochemical data, HOMO/LUMO levels, and band gaps of TDPPQ-A and TDPPQ-B.

Comp.	$E_{\text{onset}}^{\text{red}}$ (V) ^a	LUMO (V) ^b	λ_{max} (nm)	λ_{onset} (nm)	E_{g} (eV) ^c	HOMO (eV) ^d
TDPPQ-A	0.11	-4.51	638 (2-MTHF), 635 (AT)	711	1.74	-6.25
TDPPQ-B	0.11	-4.51	638 (2-MTHF), 635 (AT)	711	1.74	-6.25

^avs Ag/AgCl. All the potentials were calibrated with the Fc/Fc⁺ ($E_{1/2} = +0.43$ V measured under identical conditions). ^bEstimated from the empirical equation $\text{LUMO} = -(4.40 + E_{\text{onset}}^{\text{red}})$ eV. ^cCalculated from λ_{onset} using the formula $E_{\text{g}} = 1240/\lambda_{\text{onset}}$. ^dCalculated using the formula $\text{HOMO} = \text{LUMO} - E_{\text{g}}$.

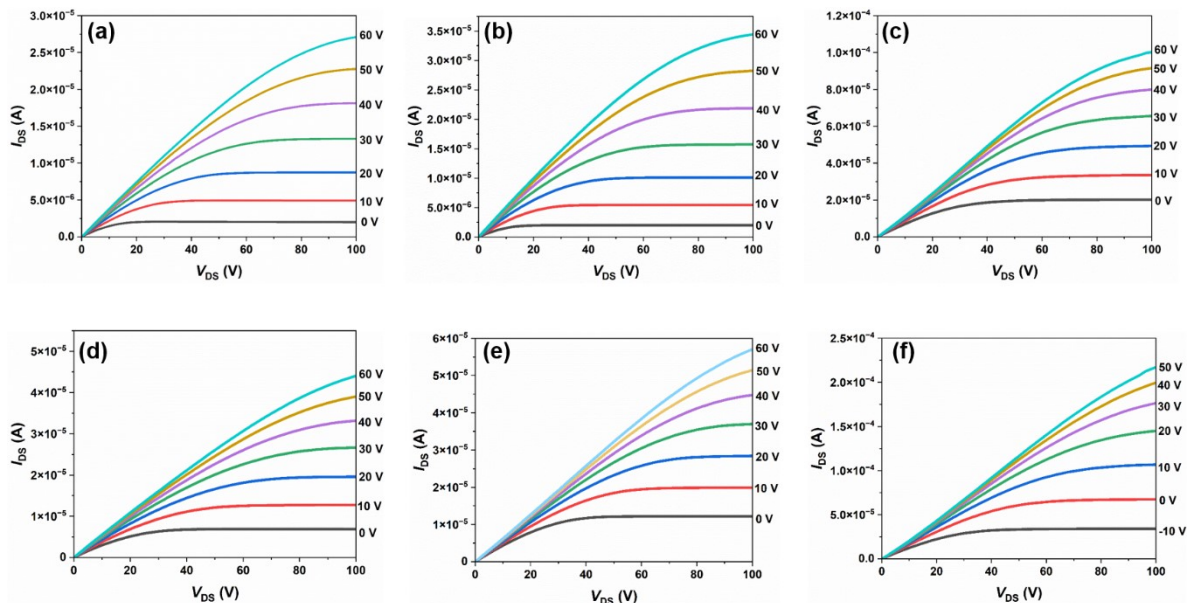


Figure S5. Output curves of the OFET devices based on (a, d) AT spin-coated films, (b, e) 2-MTHF spin-coated film, and (c, f) MTHF edge-cast films of (a, b, c) TDPPQ-A and (d, e, f) TDPPQ-B, respectively.

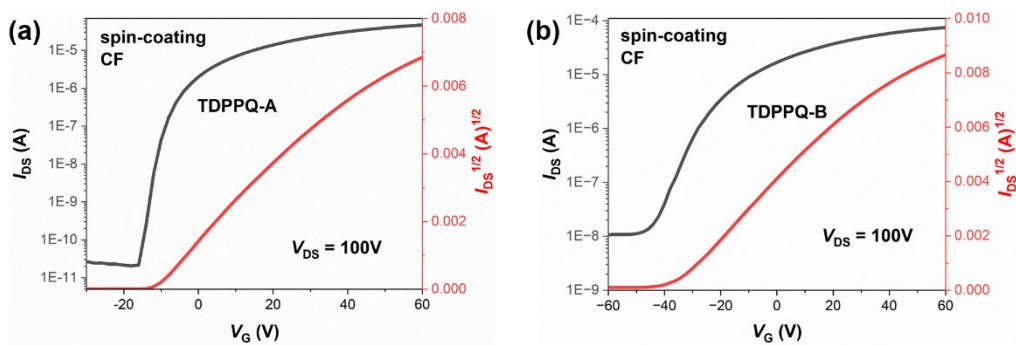


Figure S6. Transfer curves of the OFET devices based on CF spin-coated films of (a) TDPPQ-A and (b) TDPPQ-B, respectively.

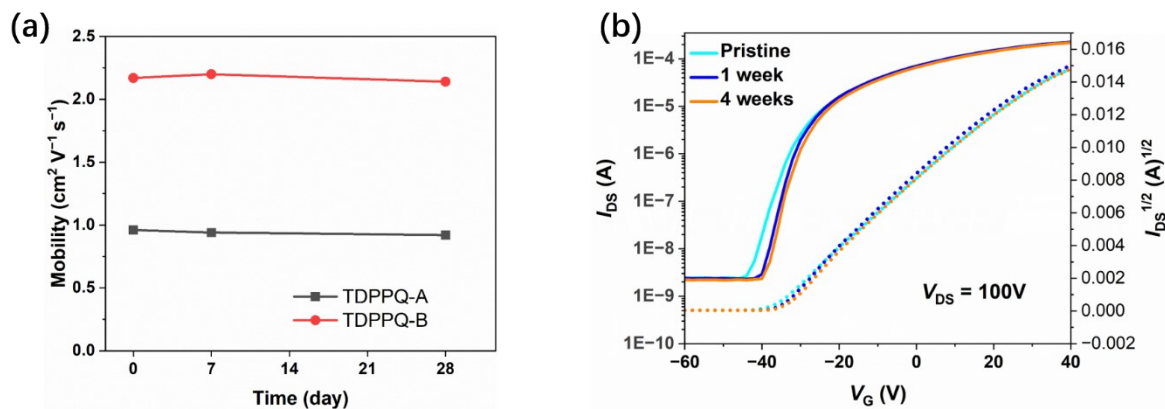


Figure S7. Long term air-stability measurements over a period of 4 weeks: (a) the change in electron mobility of devices based on edge-cast films of TDPPQ-A and TDPPQ-B, respectively; (b) the change in transfer characteristics of devices based on edge-cast films of TDPPQ-B.

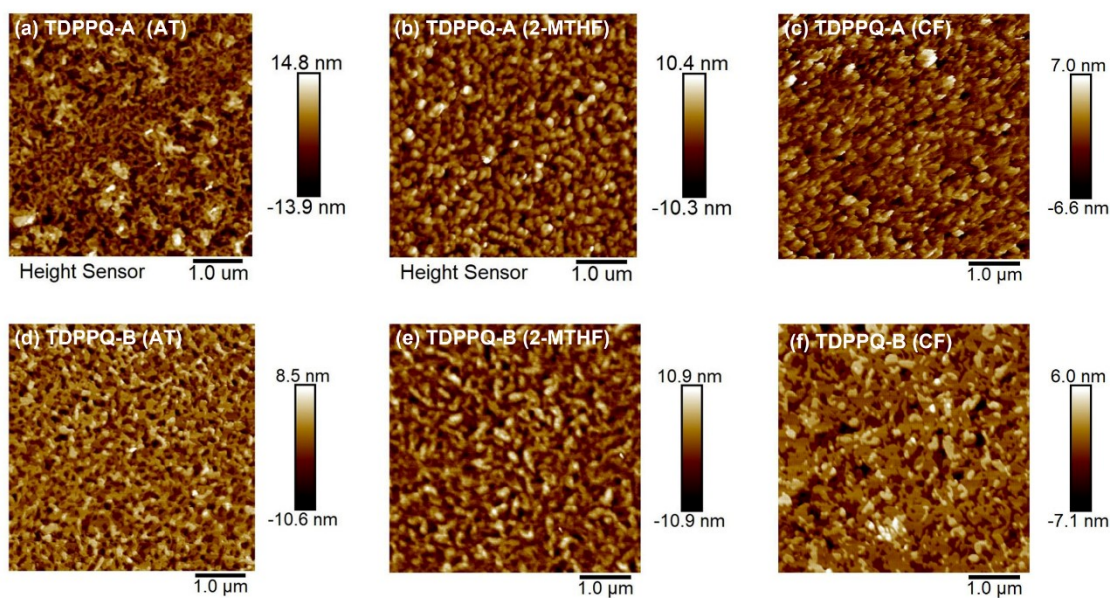


Figure S8. AFM images of spin-coated films of (a, b, c) TDPPQ-A and (d, e, f) TDPPQ-B prepared from (a, d) AT, (b, e) 2-MTHF, and (c, f) CF solutions, respectively.

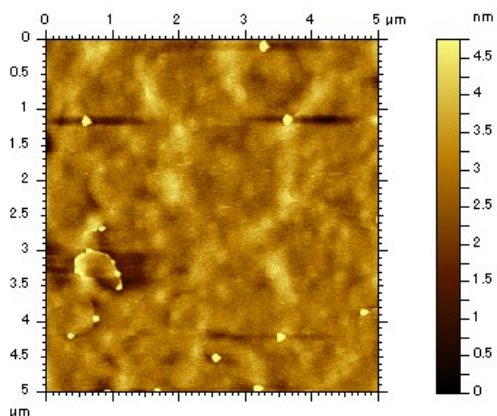


Figure S9. AFM image of 2-MTHF edge-cast film of TDPPQ-B.

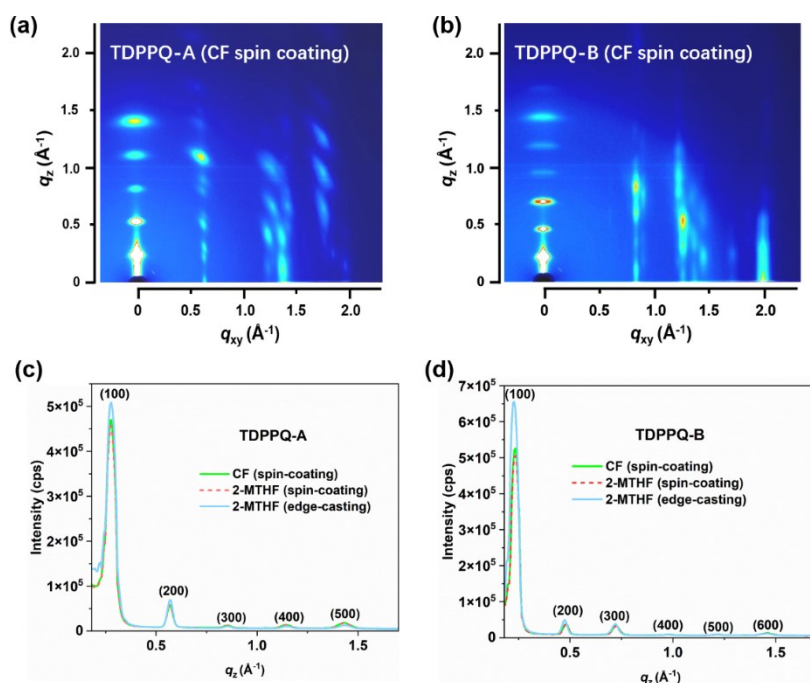


Figure S10. 2D-GIWAXS patterns of CF spin-coated films of (a) TDPPQ-A and (b) TDPPQ-B, respectively. The corresponding GIWAXS line-cut profiles of the CF spin-coated films of (c) TDPPQ-A and (d) TDPPQ-B compared to 2-MTHF processed films along the out-of-plane directions.

Table S3. The coherence length (L_c) of TDPPQ films.

Material	Solvent	Method	FWHM	L_c (nm) ^a
TDPPQ-A	AT	spin-coating	0.00113	79
	2-MTHF	spin-coating	0.000916	97
	CF	spin-coating	0.000902	99
	2-MTHF	edge-casting	0.000811	110
TDPPQ-B	AT	spin-coating	0.000797	112
	2-MTHF	spin-coating	0.000753	118
	CF	spin-coating	0.000733	121
	2-MTHF	edge-casting	0.000657	136

^a L_c was determined by GIWAXS data utilizing the Scherrer equation: $L = K\lambda/\beta \cos \theta$, where K is a constant (K = 0.89), λ is the X-ray wavelength, β is the full width at half maximum (FWHM) in radians, θ is the Bragg diffraction angle of primary peak.

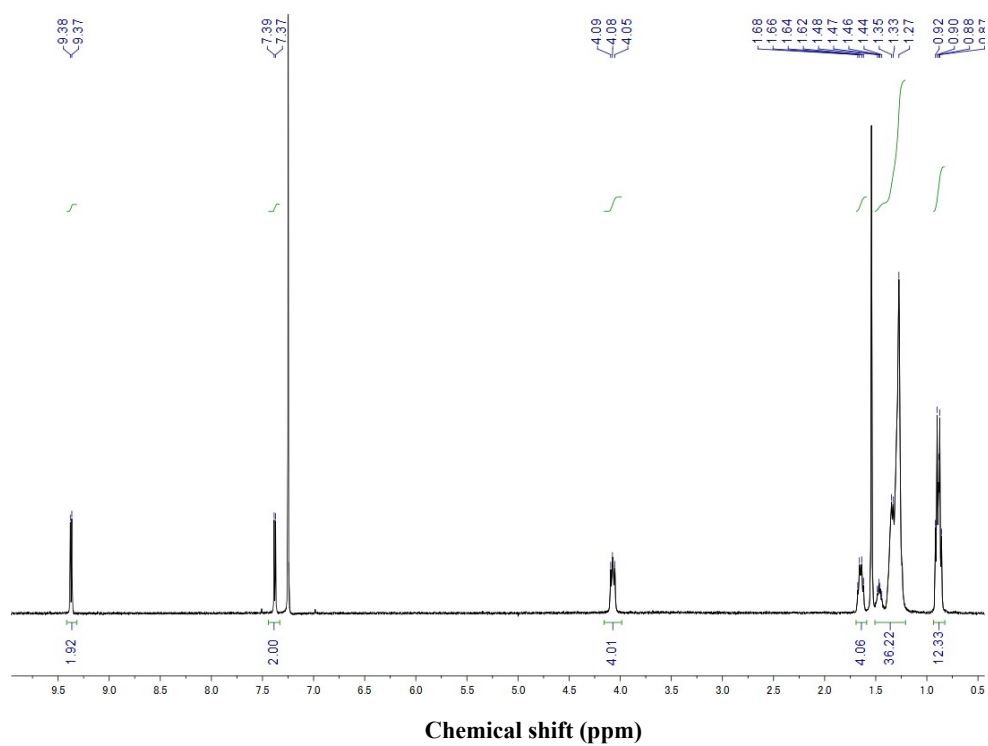


Figure S11. ^1H NMR of TDPPQ-A.

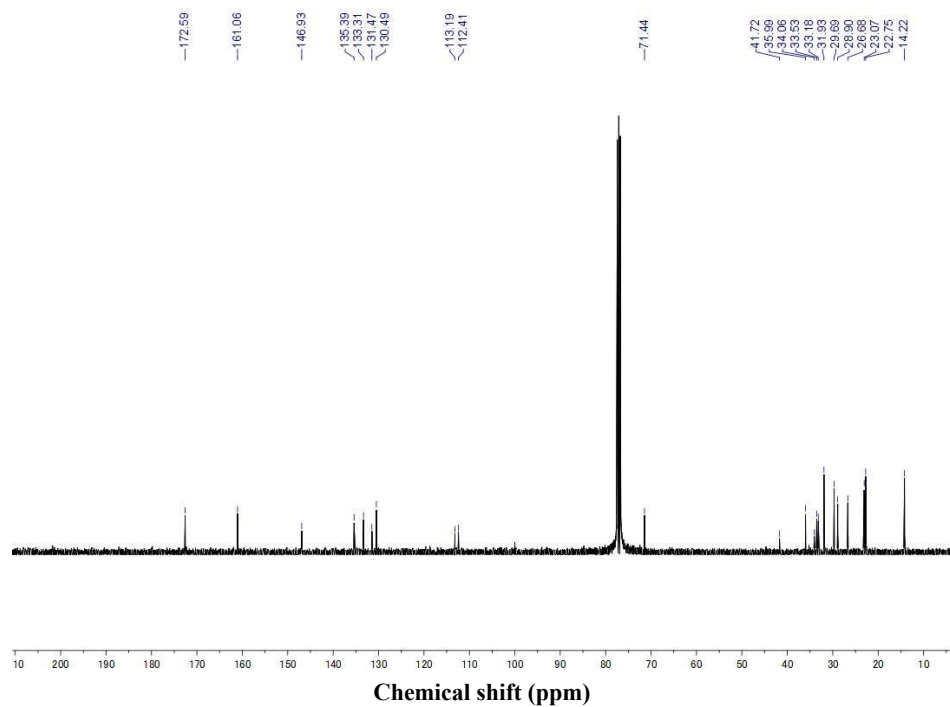


Figure S12. ^{13}C NMR of TDPPQ-A.

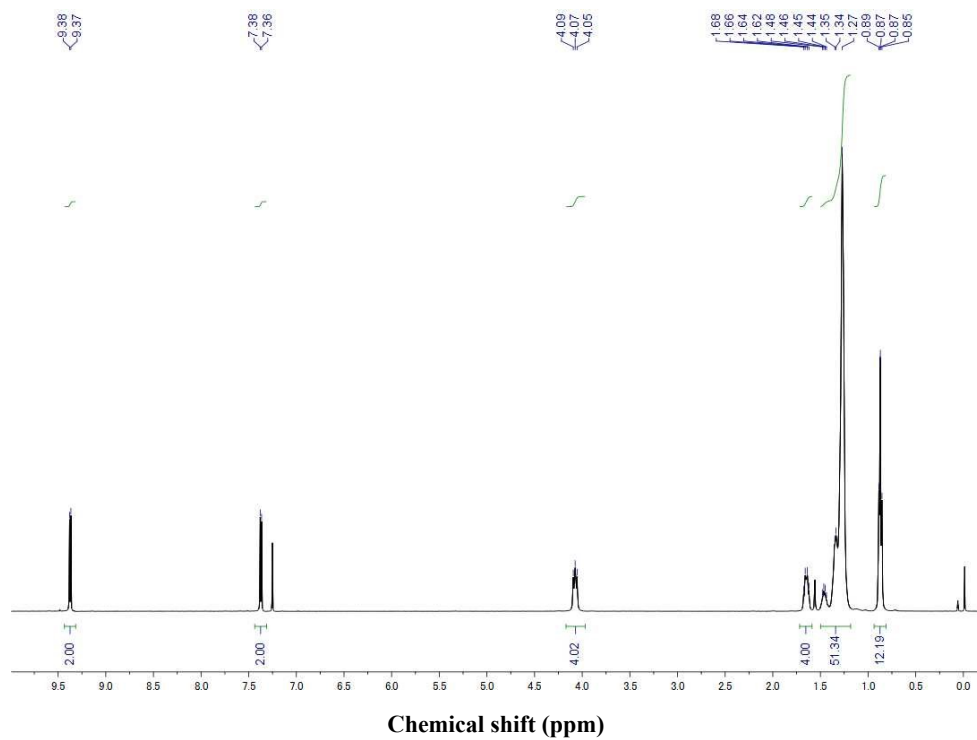


Figure S13. ^1H NMR of TDPPQ-B.

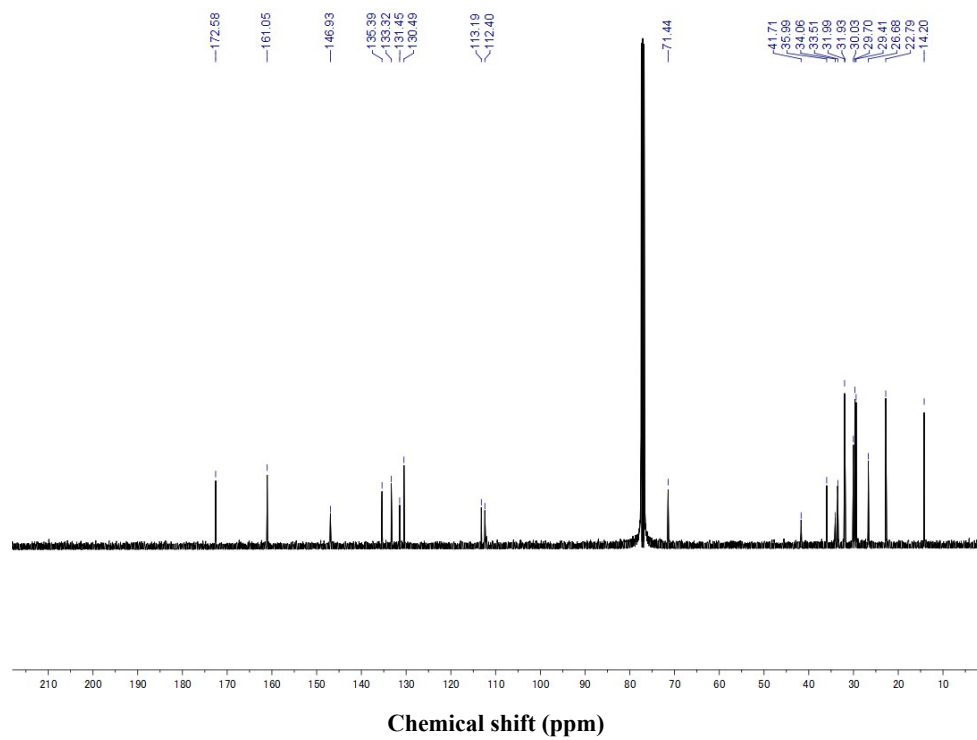
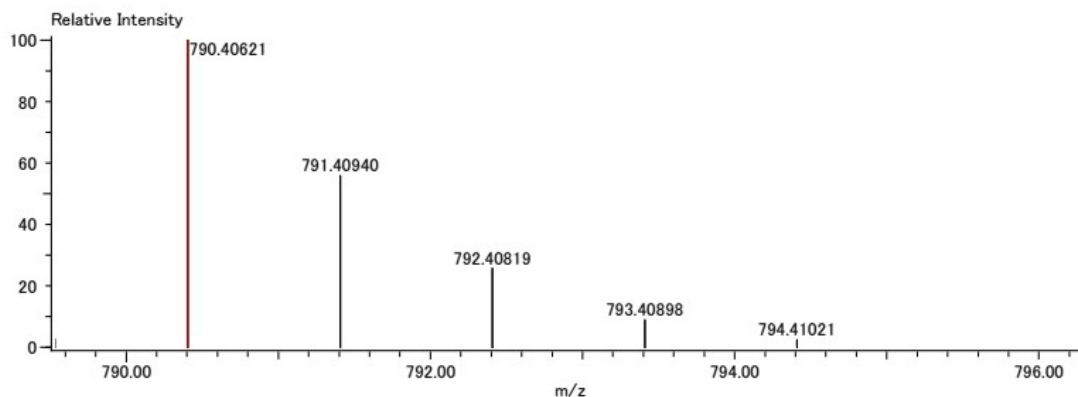


Figure S14. ^{13}C NMR of TDPPQ-B.

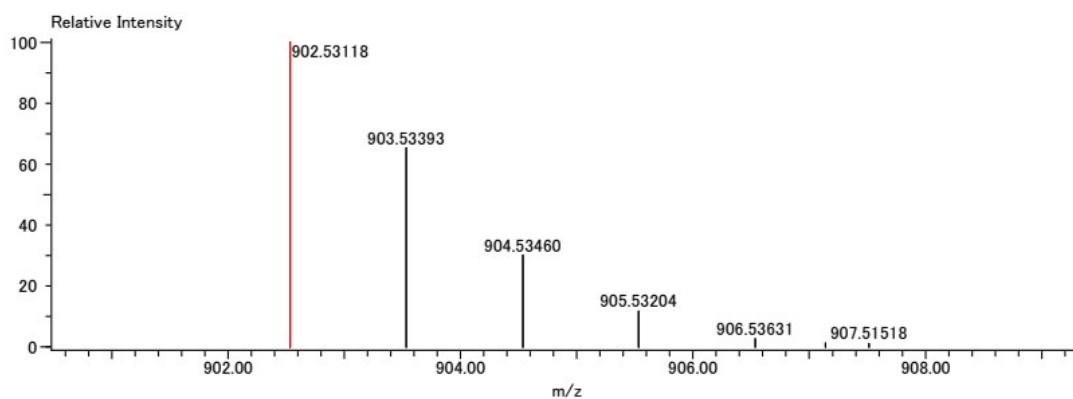
Charge number:1 Tolerance:8.00[ppm], 8.00 .. 8.00[mDa] Unsaturation Number:17.0 .. 25.0 (Fraction:Bot...
 Element:¹²C:46 .. 46, ¹H:1 .. 58, ¹⁴N:0 .. 6, ¹⁶O:0 .. 2, ³²S:0 .. 2



Mass	Intensity	Calc. Mass	Mass Difference [mDa]	Mass Difference [ppm]	Possible Formula	Unsaturation Number
790.40621	87107.68	790.40626	-0.05	-0.07	¹² C ₄₆ ¹ H ₅₈ ¹⁴ N ₆ ¹⁶ O ₂ ³² S ₂	23.0

Figure S15. HRMS of TDPPQ-A.

Charge number:1 Tolerance:8.00[ppm], 8.00 .. 8.00[mDa] Unsaturation Number:17.0 .. 30.0 (Fraction:Bot...
 Element:¹²C:54 .. 54, ¹H:70 .. 74, ¹⁴N:0 .. 6, ¹⁶O:0 .. 2, ³²S:0 .. 2



Mass	Intensity	Calc. Mass	Mass Difference [mDa]	Mass Difference [ppm]	Possible Formula	Unsaturation Number
902.53118	129374.31	902.53146	-0.29	-0.32	¹² C ₅₄ ¹ H ₇₄ ¹⁴ N ₆ ¹⁶ O ₂ ³² S ₂	23.0

Figure S16. HRMS of TDPPQ-B

Reference

- [S1] C. Wang, Y. Qin, Y. Sun, Y.-S. Guan, Wei Xu, D. Zhu, *ACS Appl. Mater. Interfaces* 2015, 7, 15978–15987.
 [S2] Y. Qiao, Y. Guo, C. Yu, F. Zhang, Wei Xu, Y. Liu, D. Zhu, *J. Am. Chem. Soc.* 2012, 134, 4084–4087.

- [S3] J. Lee, S. A. Park, S. U. Ryu, D. Chung, T. Park, S. Y. Son, *J. Mater. Chem. A* 2020, 8, 21455–21473.
- [S4] I. Deneme, T. A. Yıldız, N. Kayaci, H. Usta, *J. Mater. Chem. C* 2024, 12, 3854–3864.